MEIS study of antimony implantation in SIMOX and vacancy-rich Si(1 0 0)

M Dalponte[1], H Boudinov[1], L V Goncharova[2], E Garfunkel[2] and T Gustafsson[2]

[1] Instituto de Física, Universidade Federal do Rio Grande do Sul, 91501-970, Porto Alegre, RS, Brazil
[2] Department of Physics and Astronomy and Laboratory for Surface Modification, Rutgers University, 136 Frelinghuysen Road, Piscataway, NJ 08854-8019, USA

E-mail: mateus.dalponte@ufrgs.br

Abstract
Medium energy ion scattering was used to study the distribution of ion-implanted Sb dopant in Si with excess vacancies and separation by implanted oxygen (SIMOX) substrates and the effects of thermal treatments. Extra vacancies in Si were generated by N or O pre-implantations at high temperature. Effects related to the different chemical nature of the pre-implanted species are expected under these conditions. Different Sb annealing behaviours and distributions were observed for O and N pre-implanted Si. The oxygen-containing samples (SIMOX and O pre-implanted Si) presented higher substitutionality after long annealing times. The nitrogen pre-implanted Si presented the lowest amount of segregated Sb and more uniform dopant distribution. Both pre-implanted samples, N and O, had a large dopant loss to the atmosphere during annealing.

1. Introduction

As electronic devices reach ever higher performance and smaller power consumption, their decreasing dimensions require a better understanding of dopant behaviour during the various fabrication processes. Ion implantation is still widely used for introducing dopants into single-crystal substrates, despite the fact that this process introduces many crystal defects. It is therefore necessary to use some crystal recovery process, such as thermal annealing, to eliminate defects and to allow dopants to occupy substitutional positions in the lattice so that they can become electrically active. This procedure is likely to remain the dominant method of source/drain extension shallow junction formation in the near future [1]. In these junctions, highly doped, highly activated and low sheet resistance films must be obtained [2, 3]. The typical doping depth will be in the 10–20 nm range, which means that dopant diffusion and interaction with defects can have drastic effects on junction depth and hence on device performance [4, 5].

Heavy elements, like As and Sb, are preferred n-type dopants for Si due to their low depth penetration during ion implantation and low diffusivity during thermal treatments.

There were several reports recently showing that Sb is a strong candidate to replace As in the future devices. Sb requires a lower thermal budget to achieve the desired junction parameters when compared with As [6]. Low thermal budgets are necessary if high-κ dielectric-metal gate stacks are to be used, to avoid degradation of the material and device performance [7–9]. Sb is already being currently used for threshold voltage adjustment in 90 and 65 nm gate metal–oxide–semiconductor field-effect transistors [1].

Another approach to improve device performance is the use of defects intentionally introduced in the substrate, vacancies for example, to modify the behaviour of the dopants, like diffusivity and electrical activation. This technique has already been shown to be successful for boron [10, 11]. Vacancies are usually formed during ion implantation. de Souza *et al* [12, 13] have shown that during high temperature ion implantation in Si there are chemical effects associated with the defect formation process depending on the ion species used in the implantation (N, O, Ne or Mg). For instance, N-implanted samples presented higher compressive strain in the near surface region than O-implanted ones, which was associated with a higher vacancy

concentration. In those cases, the vacancies are expected to be mostly in the form of point defects. In the case of separation by implanted oxygen (SIMOX) they are in the form of complexes that are bonded to oxygen atoms forming vacancy-oxygen atom clusters [14]. These vacancy complexes were observed in thick SIMOX. SIMOX is one type of silicon-on-insulator material that has received great attention due to the performance improvements observed in circuits built on it and the simplicity of fabrication. It consists of a Si substrate with a buried insulating SiO_2 layer. The buried oxide (BOX) is formed by a high dose oxygen implantation followed by a long high temperature annealing. There are several types of SIMOX with varying thicknesses of the top Si film and BOX, depending on the implantation and annealing parameters. For thick SIMOX, used in our experiments, O^+ 190 keV, 1.8×10^{18} cm^{-2} implantation is used, followed by a 6 h annealing at 1300 °C [15]. The final structure consists of a 200 nm crystal Si film and a 400 nm buried SiO_2 layer on top of the Si substrate. The large oxygen dose creates the vacancies and the subsequent high temperature annealing forms the complexes.

The purpose of this work is to study Sb behaviour during high temperature treatments in Si with the presence of vacancies. Not only was the effect of the vacancies themselves analysed, but also the effect of their structures, i.e. point defects in the samples pre-implanted with nitrogen or oxygen and large complexes in SIMOX. Another effect, the chemical effects observed in the defect generation in the N and O implantations, on Sb diffusion is analysed as well. Since Sb diffusion is assisted by vacancies [16], we expect to see variations in Sb distribution depending on the vacancies structure and concentration in the substrate.

2. Experimental

The experiments were performed on (1 0 0) oriented p-type Si and thick SIMOX substrates with resistivities of 2–10 Ω cm. The native SiO_2 layer was removed in diluted HF just before implantation. In the Si samples, a 150 nm deep vacancy-rich layer was first formed by O_2^+ or N_2^+ ion implantation at 240 keV using a dose of 2.5×10^{16} cm^{-2} at 400 °C [12, 13]. Following this pre-implantation, Sb^+ was implanted at 20 keV to a dose of 5×10^{14} cm^{-2} at room temperature. The low Sb ion implantation energy guarantees that the Sb profile is fully contained in the vacancy-rich layer (the peak concentration of Sb in the as-implanted profile corresponds to a depth of ~20 nm). The samples were then processed by rapid thermal annealing (RTA) at 1000 °C for 10 s or by furnace annealing (FA) at 1000 °C for 15 min in a nitrogen atmosphere. The same Sb implantation was done in SIMOX and in a Si sample without N or O for reference. Since *all* samples were implanted with Sb, they will be labelled according to the following scheme: Si—for pure silicon without N or O pre-implantation to serve as reference sample; SIMOX—for SIMOX without N or O pre-implantation; N—for Si with N pre-implantation; and O—for Si with O pre-implantation. The thermal treatment labels can be as-implanted (not annealed), RTA or FA.

A H^+ beam with an energy of 130.5 keV was used for the medium energy ion scattering (MEIS) measurements in random and channelling alignments. Backscattered ion energies were analysed with a high-resolution ($\Delta E / E \sim 0.1\%$)

toroidal electrostatic energy detector resulting in a depth resolution of ~0.9 nm at a depth of 50 nm. The double alignment geometry was used in all channelling measurements to minimize the signal from the Si substrate. The beam was aligned in the [1 0 0] channelling direction and the detector position was centered on the [1 1 1] blocking direction, at a scattering angle of 125.5°. For the random geometry measurements, the sample was rotated in the sagittal plane in such a way that the incident beam was directed 9.5° off the sample normal, but the backscattering angle remained constant. The surface approximation [17] with energy loss values extracted from the software SRIM [18] was used to convert the energy scale of the spectra into depth scale. A well-known relation between backscattering yield and concentration [17] was used to determine the dopant concentration profile and, hence, estimate the metallurgical p–n junction depth (depth at which the implanted dopant concentration equals that of the substrate doping) for a substrate doping of 1×10^{18} cm^{-3}, after smoothing the concentration profiles.

3. Results and discussion

The Sb peaks in selected MEIS energy spectra in random alignment are shown in figure 1. The Sb profile in the as-implanted sample is also shown for reference. Only one as-implanted Sb distribution is shown since there was no observable difference between the samples before RTA/FA, i.e. the Sb implantation distribution is not affected by the N or O pre-implantations.

After RTA (figure 1(*a*)), there is a small broadening of the dopant distribution in comparison with the as-implanted profile. Diffusion towards the bulk of the sample (higher number of counts in the annealed samples for energies below 119 keV when compared with the as-implanted one) as well as towards the surface (appearance of peaks at energies around 126.5 keV after annealing) is observed. The SIMOX sample shows a peak (around 126.5 keV) related to Sb segregation at the interface between the Si substrate and the native surface SiO_2. The same feature, but with much lower intensity, was observed in the other samples too.

In the FA samples (figure 1(*b*)), the situation is completely different. A large amount of Sb ($(0.8–1.5) \times 10^{14}$ atoms cm^{-2}) segregates at the interface with the native oxide, as can be seen by the presence of distinct surface peaks for all samples (around 126 keV). The dopant loss increases as well, reaching the highest value in the samples that were pre-implanted with N or O, the O one being the worst case, with about 34% dopant loss, followed by N with 19%. The dopant loss in Si and SIMOX is much lower; even after the long annealing it is only 2% and 5%, respectively. The dopant loss percentage was calculated as 1 minus the ratio of Sb areal density for the annealed samples to the as-implanted ones, which corresponds to 1 minus the retained dose. Very small dopant loss is observed in the RTA samples (see figure 2(*a*)). The metallurgical junction depth, which was 33 nm in the as-implanted sample (at 118.5 keV in figure 1(*a*)), increased after a short annealing (at 117.6 keV for O and N samples and 117 keV for SIMOX), but decreased during the long annealing in all samples (at 119.3 keV for O and N samples and 118.9 keV for SIMOX). Figure 2(*b*) shows a plot of junction depth variations. The final value was even smaller
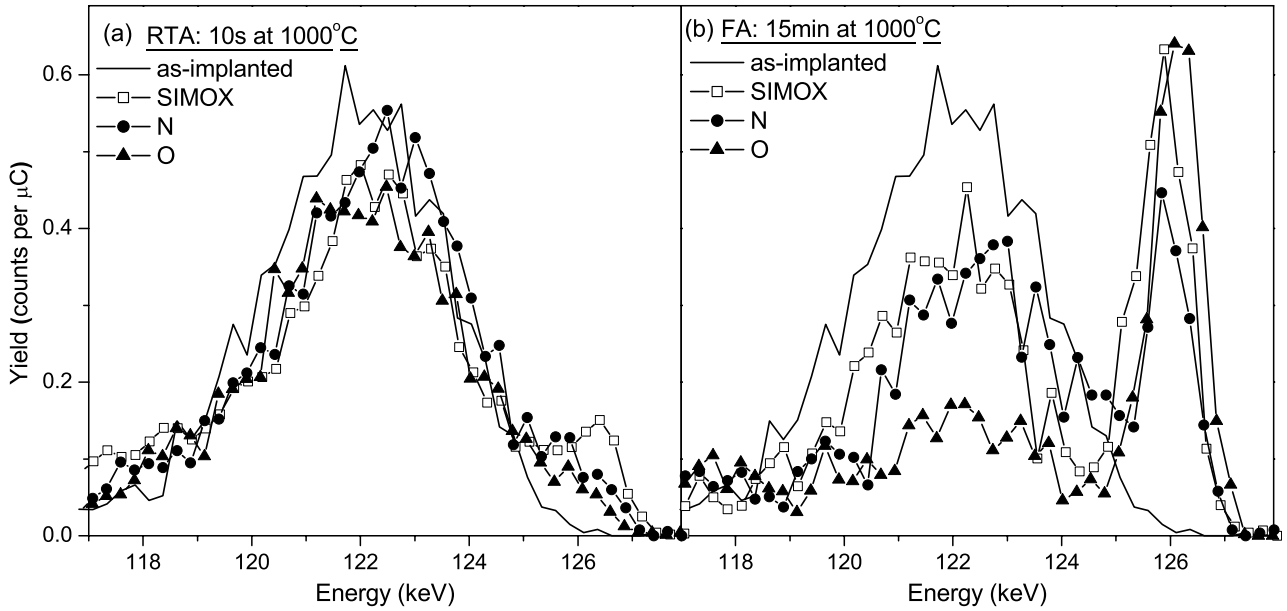
Figure 1. Selected MEIS spectra in random alignment of annealed samples. As-implanted sample data is shown by a solid line for reference. (*a*) After RTA, diffusion towards the surface and the bulk of the substrate is observed. Sb begins to segregate at the interface with the native oxide, especially in the SIMOX sample. (*b*) After FA, a larger Sb peak at SiO_2/Si interface (around 126 keV) shows more segregation. Sb is diffusing towards the sample bulk and surface (see both low and high energy tails of the spectra, respectively).
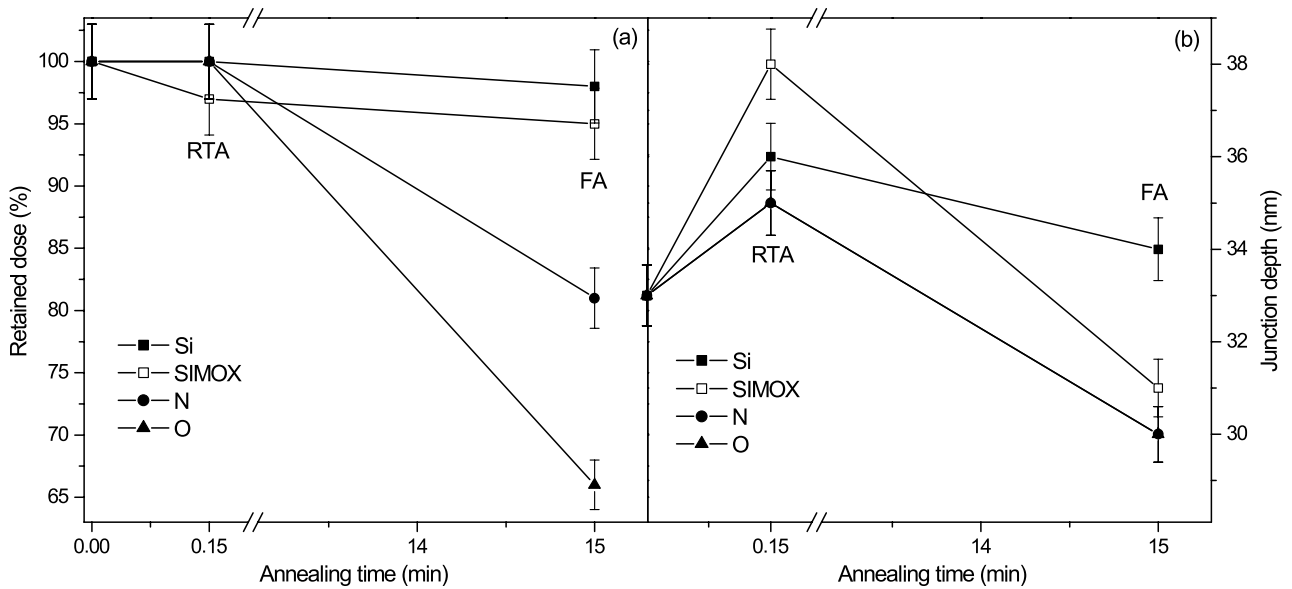
Figure 2. Retained dose (*a*) and junction depth (*b*) as a function of annealing time at 1000 °C.

than the initial in all samples except Si. A similar effect was observed by others [6]. The dopants are pushed out during solid phase epitaxy. The N or O pre-implanted samples presented the shallowest junctions after both annealings. Considering that they also had the highest dopant loss, it is likely that the defects generated during the pre-implantation are enhancing dopant diffusion towards the surface and preventing it from diffusing deeper into the substrate.

Figure 3 shows the Sb peaks for the annealed samples in channelling alignment. In this alignment, only the atoms in interstitial (non-substitutional) positions or in amorphous structures are detected by the beam. The spectrum for the as-implanted sample is also shown for reference.

The as-implanted spectra in the silicon energy range in random and channelling alignment (not shown) were identical, indicating that the Sb implantation amorphized the top layer of the sample, from the surface to a depth of ∼32 nm. It also indicates that the vacancies do not play any role in the accumulation of ion implantation-generated defects. Also, the surface Sb peaks are similar for all samples in the channelling and random alignments, indicating that the Sb located at the SiO_2/Si interface is not substitutional. This region of the spectra where the surface peaks in channelling and random alignment coincide was defined as the segregated Sb. In channelling alignment the substitutional Sb atoms are not visible, hence the peak of the segregated atoms at the SiO_2/Si interface
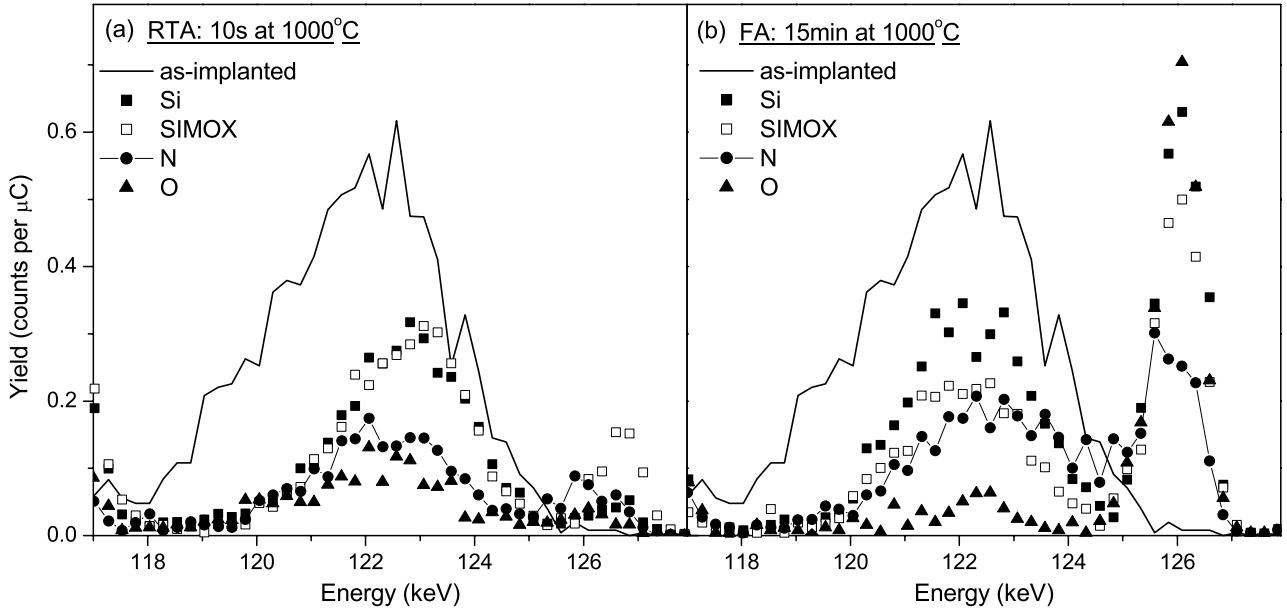
Figure 3. MEIS spectra in channelling alignment. The as-implanted samples data are shown for reference. Only the non-substitutional Sb atoms are visible. The segregated Sb peaks can be seen more clearly in this geometry. A large increase in segregated Sb can be seen comparing the RTA annealed samples (*a*) with the FA annealed ones (*b*).
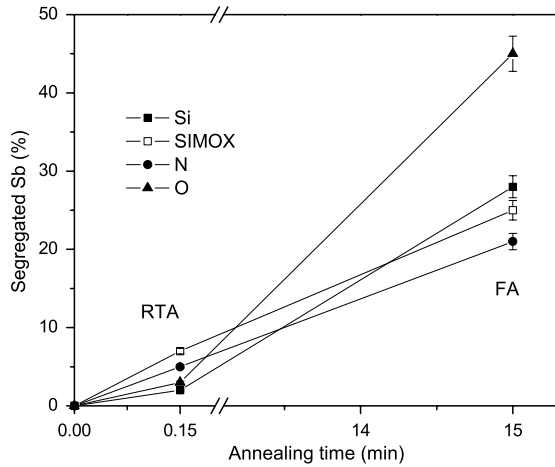
Figure 4. Segregated Sb percentage as a function of annealing time.

can be resolved more clearly. The segregation percentage was calculated as the ratio of the Sb areal density in the surface peak of the channelling spectrum to the total Sb areal density (whole random spectrum) for the corresponding sample. Figure 4 shows the evolution of the segregated Sb percentage with annealing time. After the short annealing (RTA), the segregation effects are small. It is most pronounced in the SIMOX and N samples. After a long annealing (FA), there is a huge increase of the segregated Sb peak (see figure 3(*b*)). The Si and SIMOX samples presented very similar segregation percentages, while N had the lowest and O had the highest value. In the N sample, nitrogen was accumulated at the interface (a nitrogen peak was observed, not shown). Nitrogen usually works as a diffusion barrier, which should be the reason for a lower dopant loss when compared with the O sample and less segregation than what was observed for the other samples. Nitrogen was detected at the SiO_2/Si interface only in the FA sample.

The percentage of substitutional Sb atoms can be obtained comparing the random and channelling spectra for each sample. Figure 5 shows the spectra of SIMOX after (*a*) RTA and (*b*) FA as an example. Similar features are observed in the spectra of the other samples. The difference between the normalized random and channelling spectra accounts for the atoms that are invisible to beam, i.e., in substitutional positions. Note that the surface peaks are similar in both alignments. In the low energy tail of the surface peaks in figure 5(*b*) the random yield is higher than the channelling due to substitutional Sb atoms right beneath the ones that are segregated. The substitutional percentage was defined here as 1 minus the ratio of the integrated area of the Sb peak in channelling alignment to the respective peak area in random alignment in the ∼119–125 keV energy range, e.g. *excluding* the surface peak. This gives the substitutionality of the Sb atoms that are not segregated. In figure 6, the substitutionality is plotted as a function of annealing time. O samples have the highest substitutionality, but they also had the highest dopant loss. It is not surprising that a lower dopant amount can be accommodated more easily in the Si crystal lattice. It is interesting to note that after a short annealing the substitutionality in the N and O samples was higher than in Si and SIMOX. The vacancies generated in the pre-implantation step are increasing the dopant incorporation into the lattice. Sb substitutionality in the two oxygen-containing samples (SIMOX and O) is improving after the long annealing, while the opposite behaviour is observed in Si and N samples. The Sb electrical deactivation in Si by becoming non-substitutional is a well-known effect [19]. The N sample shows the same behaviour as Si with a similar rate. The different trend presented by the SIMOX and O samples might be related to chemical specificity of oxygen interaction with vacancies and the dopant itself.

After the short annealing (RTA), the N and O samples had no significant dopant loss, the shallowest junctions and
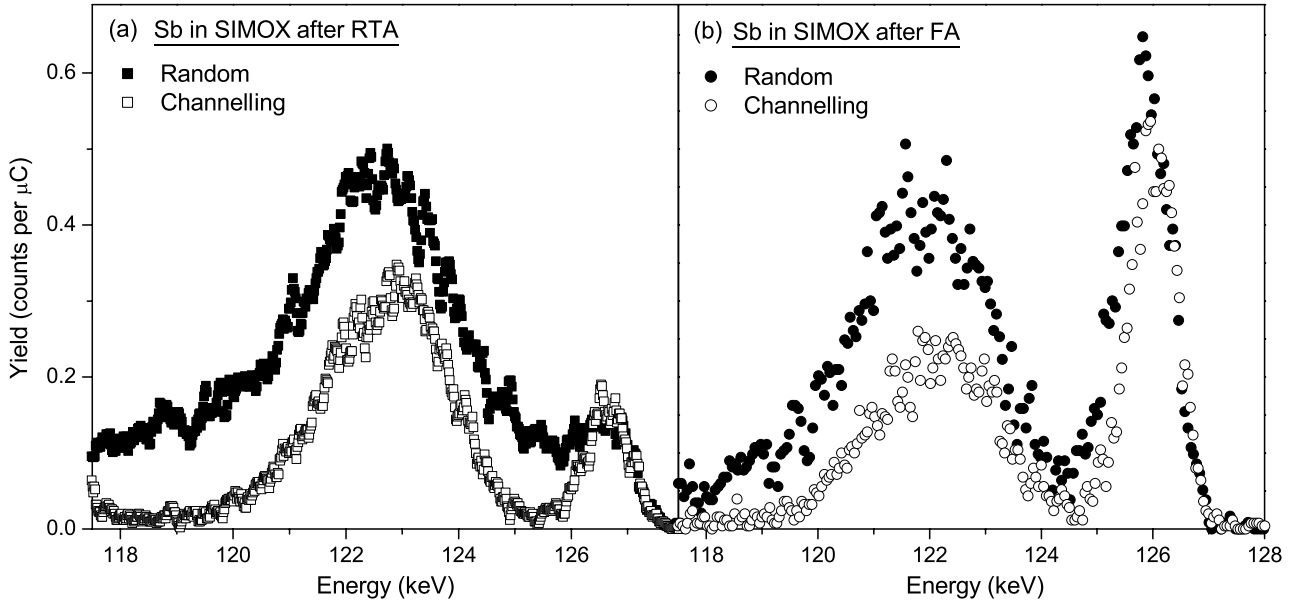
Figure 5. Random and channelling spectra of SIMOX after RTA (*a*) and FA (*b*). The segregated Sb peak corresponds to the area where the surface peaks in random and channelling alignments coincide. The difference in the area of the random to the channelling spectra for energies below the segregated peak is proportional to the dopant substitutionality.
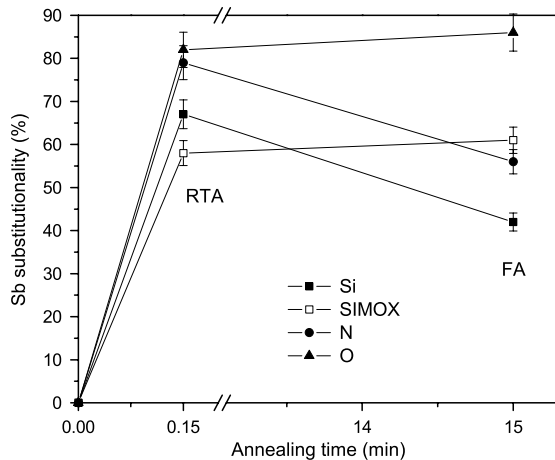
Figure 6. Sb substitutionality as a function of annealing time. Oxygen-containing samples presented an increase in substitutionality after a long annealing, which is the opposite behaviour normally observed in silicon.

the highest dopant substitutionality. The vacancies created during the pre-implantation most likely promote an easier incorporation of the dopants into the crystal lattice, decreasing their loss and diffusion deeper into the substrate (smallest change in junction depth). No chemical effects were observed at this stage. On the other hand, SIMOX, which also contains excess vacancies, had the highest dopant loss and segregation, deepest junction and lowest substitutionality. These apparent discrepancies can be understood by considering the structure of the vacancies in these samples. In the N and O samples the vacancies exist as point defects because they had just been created by the pre-implantation and have not been annealed prior to the dopant implantation. In SIMOX the vacancies are in the form of clusters surrounded by oxygen atoms [11], which makes them much less mobile and reactive. These vacancy complexes are formed during the SIMOX fabrication

annealing at 1300 °C for 6 h. When the dopant is implanted, these complexes are already much more stable than the point defects found in the N and O samples.

The Si sample results were in between the ones of the SIMOX and those of the N and O samples. Considering Si as a reference material, this tells us that in the same way that the point defects in the N and O samples increase Sb substitutionality and decrease dopant loss and segregation, the vacancy-oxygen complexes in SIMOX have the opposite effect. It seems that the vacancy complexes in SIMOX only increase Sb diffusivity without making them substitutional, i.e. they act as 'diffusion catalysts' as opposed to the point defect-type vacancies in the N and O samples that capture the dopant atoms.

After the long annealing (FA), the Si sample shows the highest stability in terms of dopant loss and variation of junction depth, due to the absence of excess vacancies, since Sb is a vacancy-assisted diffuser. There was, however a large increase in segregation, decrease in substitutionality and a net Sb diffusion towards the surface.

Effects of the chemical specificity of N and O interactions with the dopant are observed. The opposite trend in the substitutionality as a function of annealing time for the samples with (SIMOX and O) and without (Si and N) oxygen suggests that oxygen facilitates the Sb incorporation into the crystal lattice. It is possible that this is only a transient effect and that Sb will start to become non-substitutional after longer annealing times and substitutionality begins to follow the trend observed in the other samples. Further experiments with longer annealing times are necessary to verify this hypothesis. The increase in Sb substitutionality of the O sample should not be exclusively related to the dopant loss since the N sample had a larger dopant loss than SIMOX and its Sb substitutionality decreased after a long annealing. O sample dopant segregation is the highest of all, which might have led to the highest dopant loss. On the contrary, the N sample also had a large dopant loss, but the lowest segregation. The nitrogen accumulation

at the SiO$_2$/Si interface should have partially prevented Sb outdiffusion when compared with the O sample (same point defect-type vacancies) and segregation when compared with all samples. The major cause of dopant loss seems to be the presence of vacancies in the form of point defects. Similar Sb net diffusion towards the surface as observed in the Si sample is observed in the other samples; however, different effects have to be considered. In figure 1(*b*) we see Sb distribution is more uniform in the N sample than in the other samples. Most of the samples (except N) have a two-layered structure, consisting of the segregated Sb layer and the layer with the dopants remaining near their initial as-implanted distribution. In the N samples, a similar but less pronounced structure is observed, i.e. there is more Sb in the intermediate region between the peaks than in the Si, SIMOX and O samples, which should be preventing dopant segregation at the SiO$_2$/Si interface. The presence of nitrogen at the interface rejects the dopant from that region.

4. Conclusions

MEIS was used to study Sb behaviour in Si with excess vacancy concentration generated by N or O high temperature pre-implantation and SIMOX substrates. For a short annealing time, both N and O pre-implanted samples presented the highest substitutionality and the shallowest junctions. Low dopant loss and dopant segregation to the SiO$_2$/Si interface was observed in all samples. After a long annealing, several effects related to the nature of the defects present in the sample as well as to the pre-implantation species became apparent. The percentage of dopant loss seems to be related to the structure of the defects. The highest dopant loss percentages were observed in the N and O pre-implanted samples, where the vacancies had a point defect character. In Si (no excess vacancies) and SIMOX (vacancies in the form of stable complexes) the dopant loss was much lower than in the N and O samples.

Chemical effects were also noticed. The samples containing oxygen, SIMOX and Si with pre-implanted oxygen have shown an opposite trend in the substitutionality as a function of annealing time compared with the samples without oxygen. The substitutionality of the former ones was still increasing after a long annealing, while in the other samples it was decreasing at a higher rate. Hence, oxygen is likely to facilitate Sb incorporation into the Si lattice.

The N samples had the lowest segregated Sb percentage. While in the other samples the Sb formed a two layer structure (the atoms segregated at the SiO$_2$/Si interface and the atoms near their initial as-implanted distribution), in the N sample the Sb is more uniformly distributed and this structure is less pronounced. However, this effect does not completely prevent dopant loss. The nitrogen accumulating at the SiO$_2$/Si interface

decreased dopant loss when compared with the O samples (same vacancy structure) and segregation when compared with all the other samples.

To summarize, point defect-type vacancies increase dopant loss, oxygen increases substitutionality after long annealing times and nitrogen decreases dopant loss and segregation at the interface with the native oxide.

References

[1] 2005 *International Technology Roadmap for Semiconductors* Semiconductor Industry Association International SEMATECH Austin TX, USA
[2] Kim S-D, Park C-M and Woo J C S 2002 *IEEE Trans. Electron Devices* **49** 1748
[3] Uedono A, Chen Z Q, Ogura A, Suzuki R, Ohdaira T and Mikado T 2002 *J. Appl. Phys.* **91** 6488
[4] Jones C and Ishida E 1998 *Mater. Sci. Eng.* R **24** 1
[5] Chen Z Q, Uedono A, Ogura A, Ono H, Suzuki R, Ohdaira T and Mikado T 2002 *Appl. Surf. Sci.* **194** 112
[6] Tavakoli S G, Baek S, Chang H S, Moon D W and Hwang H 2004 *Electrochem. Solid State Lett.* **7** G216
[7] Watanabe H and Ikarashi N 2002 *Appl. Phys. Lett.* **80** 559
[8] Copel M, Cartier E, Gusev E P, Guha S, Bojarkzuk N and Poppeller M 2001 *Appl. Phys. Lett.* **78** 2670
[9] Goncharova L V, Dalponte M, Starodub D G, Gustafsson T, Garfunkel E, Lysaght P S, Foran B, Barnett J and Bersuker G I 2006 *Appl. Phys. Lett.* **89** 044108
[10] Shao L, Zhang J, Chen J, Tang D, Thompson P E, Patel S, Wang X, Chen H, Liu J and Chu W-K 2004 *Appl. Phys. Lett.* **84** 3325
[11] Smith A J, Colombeau B, Gwilliam R, Cowern N E B, Sealy B J, Milosavljevic M, Collart E, Gennaro S, Bersani M and Barozzi M 2005 *Matter. Sci. Eng.* B **124–125** 210
[12] de Souza J P, Suprun-Belevich Yu, Boudinov H and Cima C A 2000 *J. Appl. Phys.* **87** 8385
[13] de Souza J P, Suprun-Belevich Yu, Boudinov H and Cima C A 2001 *J. Appl. Phys.* **89** 42
[14] Kruseman A C, Schut H, van Veen A and Fujinami M 1999 *Nucl. Instrum. Methods* B **148** 294
[15] Colinge J P 1997 *SOI Technology: Materials to VLSI* (Dordrecht: Kluwer Academic)
[16] Fahey P M, Griffin P B and Plummer J D 1989 *Rev. Mod. Phys.* **61** 289
[17] Chu W-K 1978 *Backscattering Spectrometry* (New York: Academic)
[18] Ziegler J F and Biersack J P 2003 *SRIM: The Stopping and Range of Ions in Matter* version 2003.26, http://www.srim.org
[19] Takamura Y, Vailionis A, Marshall A F, Griffin P B and Plummer J D 2002 *J. Appl. Phys.* **92** 5503